We appreciate the valuable comments and constructive suggestions provided by referees, which have greatly helped us improve the quality of this manuscript. Our responses (blue text) are presented below.

Response to Referee 1

This paper describes some dramatic variations of the mesospheric Na layer during a night, captured by a Na lidar. To understand the underlying mechanism, simultaneous observations from a nearby meteor wind radar and ionosonde are introduced. The results are consistent with those reported by the previous studies, and the paper is mostly clean and easy to follow. This important work demonstrates the complexity of the dynamics in the mesosphere and lower thermosphere, which is reflected by the mesospheric Na variations. While the description of the event is straight forward, some of the critical terminologies need more rigorous definition and clarification. For example, the definition of SSL is quite vague and there is no definition of ESP at all in the paper. I would like to see some rigorous quantitative definitions for these two features that discussed intensively in the paper. This will clarify the ambiguity on why the event between ~18:30 and 19:30 is not qualified as SSL but, instead, an ESP? Both have the similar thickness, except the peak Na number density of ESP is less than that of SSL. It appears the categorization is related to the comparison between the instantaneous Na profile and the background Na. However, the calculation process of this background Na profile is not described. The altitude of Es (what is h'Es?) is also not defined. The arguments on the Es being the primary source of SSL1 and SSL2, along with the role of horizontal wind, are also not convincing. The author reaches this conclusion based on "The close spatiotemporal correspondence between SSL and Es". However, the two events are ~ 10 km apart in altitude, meaning the electron number density near the SSL could be very low, depending on the thickness of Es. There is no horizontal wind data in the Es altitudes. Thus, the zero-wind line argument is just a pure hypothesis. One potential argument regarding these two issues could be the different tracers of ionosonde and the lidar. The ionosonde measures echoes from electrons, not the Na+, which could converge at lower altitude (Kopp, 1997). None the less, I would tune down these two statements throughout the paper.

Thank you for these valuable comments. We have revised the manuscript accordingly.

1. Quantitative definitions of SSL and ESP

We have revised the manuscript (Lines 80–88) to provide quantitative identification criteria for SSLs and ESPs. In this study, the identification of SSLs follows the criteria proposed by Dou et al. (2009):

(1) The peak sodium density of the SSL must be at least twice the background sodium density at the same altitude and exceed 1000 cm^{-3} when the SSL occurs above 100 km.

(2) The full width at half maximum (FWHM) of the layer must be less than 4.0 km.

(3) The layer must persist for at least four successive lidar profiles (more than 16 min in Dou et al., 2009).

In our study, the sodium density observations have a temporal resolution of 1 min. Therefore, the third criterion was modified accordingly, and an SSL is required to persist for at least 15 consecutive profiles (15 min). This modification preserves the same physical duration criterion while accounting for the higher temporal resolution of our observations.

An ESP is defined as an obvious sodium density enhancement event that does not satisfy one or more of the above SSL identification criteria.

For the enhancement observed between 18:30 and 19:30 UT shown in Figure R1, we classify it as an ESP rather than an SSL for two reasons. First, the preceding SSL event (17:00–18:00 UT) was clearly interrupted at approximately 18:15 UT. Therefore, the enhancement beginning at 18:30 UT is regarded as a new sodium enhancement event rather than a continuation of the previous SSL. Second, although this enhancement is clearly distinguishable from the background sodium layer, its peak sodium density does not reach twice the background sodium density at the same altitude and therefore does not satisfy the first SSL identification criterion. Consequently, it is classified as an ESP rather than an SSL.

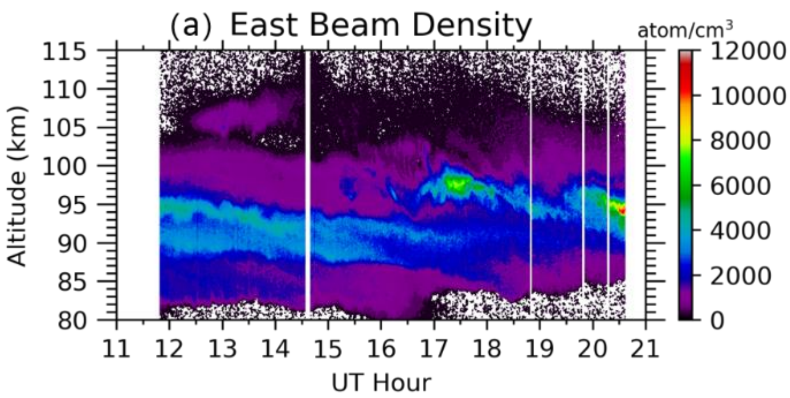

Figure R1. Time–height contours of east beam sodium density between 11:00 and 21:00 UT, 13 June 2013. The white vertical lines represent data gaps.

Reference:

Dou, X. K., Xue, X. H., Chen, T. D., Wan, W. X., Cheng, X. W., Li, T., Chen, C., Qiu, S., and Chen, Z. Y.: A statistical study of sporadic sodium layer observed by Sodium lidar at Hefei (31.8° N, 117.3° E), Ann. Geophys., 27, 2247–2257, https://doi.org/10.5194/angeo-27-2247-2009, 2009.

2. Background sodium profile

We have added a description of the background sodium profile determination procedure in Lines 89-93 of the revised manuscript.

The background sodium profile used for SSL identification is determined iteratively. The all-night averaged sodium density profile is first adopted as the initial background profile. Sodium density profiles whose sodium densities exceed twice the background value are regarded as containing SSLs and are excluded from the background calculation. The remaining profiles are averaged to obtain an updated background profile, and the procedure is repeated until the background profile converges. The converged profile is used as the final background sodium profile.

3. Definition of h′Es

We have added a definition of h′Es in the revised manuscript (Lines 105-106). Specifically, h′Es denotes the virtual reflection height (virtual height) of the sporadic E layer derived from ionograms.

4. Interpretation of the relationship between Es, SSLs, and horizontal wind

We agree that the present observations provide supporting evidence rather than conclusive proof of a causal relationship. Accordingly, we have toned down the corresponding statements throughout the manuscript. For example, the statements at Lines 254-256 have been modified.

Minor technical issues:

1. Line 61, please define ESP

We have added the definition of SSL and ESP at Lines 80–88 of the revised manuscript. And the ESP is defined as an obvious sodium density enhancement event that does not satisfy one or more of the SSL identification criteria.

2. Line 75, regarding the uncertainties, are these values including both statistical and systematic uncertainties?

The uncertainties presented in the manuscript are derived from photon noise and laser frequency locking fluctuation, following Li et al. (2012). Photon noise represents the dominant statistical uncertainty, whereas laser frequency locking fluctuation represents an instrumental uncertainty associated with the lidar system. We have clarified this point at Lines 76-77 in the revised manuscript.

Reference:
Li, T., Fang, X., Liu, W., Gu, S., and Dou, X.: Narrowband sodium lidar for the measurements of mesopause region temperature and wind, Appl. Opt., 51, 5401–5411, https://doi.org/10.1364/AO.51.005401, 2012.

3. Line 95, “upward propagation” and the “downward propagation” used later in line 115 are referring to the feature of the atmospheric waves. The SSLs are not waves feature and, thus, these terminologies do not fit the description here. Same for the ESP description in line 139, using “downward phase propagation”.

We agree that the terms upward propagation, downward propagation, and downward phase propagation are more commonly used to describe wave phenomena and may not be appropriate for SSLs and ESPs. Accordingly, we have revised the relevant terminology throughout the manuscript. Following the terminology adopted by Dou et al. (2009), “upward/downward propagation” and “downward phase propagation” have been replaced with “upward/downward motion”. For example, the corresponding revisions can be found in the revised manuscript (Lines 111, 132, and 156).

Reference:
Dou, X. K., Xue, X. H., Chen, T. D., Wan, W. X., Cheng, X. W., Li, T., Chen, C., Qiu, S., and Chen, Z. Y.: A statistical study of sporadic sodium layer observed by Sodium lidar at Hefei (31.8° N, 117.3° E), Ann. Geophys., 27, 2247–2257, https://doi.org/10.5194/angeo-27-2247-2009, 2009.

4. Line 150-155, the determination of the black dashed lines in Figure 5 seem somewhat arbitrary. Please provide clarification on how they are decided or calculated.

Thank you for this comment. We have clarified the determination of the black dashed lines at Lines 169-173 and the caption of Figure 5 in the revised manuscript and here use the Figure R2 to illustrate the procedure.

As shown in Figure R2, the white solid lines represent the altitude variations of the peak sodium density associated with each ESP event. The black dashed lines correspond to the trajectories shown in Figure 5 of the manuscript, while the red dotted lines denote linear fits to the peak-density altitude variations.

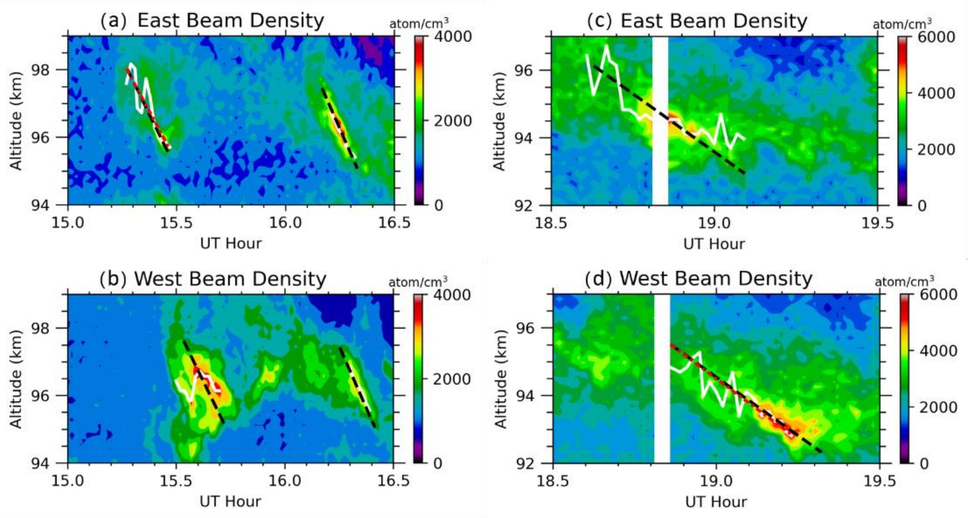

Figure R2. Time–height contours showing the detailed structures of ESP1 and ESP2 (a, b) and ESP3 (c, d) observed by the east beam (a, c) and west beam (b, d). The white solid lines indicate the altitude variations of the maximum sodium density during each ESP event. The red dotted lines represent linear fits to the white solid lines. The black dashed lines correspond to the trajectories presented in Figure 5 of the manuscript and closely follow the red dotted lines, suggesting that they could be used to illustrate the evolution of the ESP features.

For ESP1, the sodium density variations in the west beam exhibit relatively complex structures. Therefore, the altitude variation of the peak sodium density derived from the east beam is used to characterize the overall evolution of ESP1 in both beams. As shown in Figure R2(a), the fitted trajectory derived from the east beam agrees well with the trajectory presented in Figure 5 and provides a reasonable representation of the corresponding feature in the west beam.

For ESP2, the trajectories shown in Figure 5 are directly determined from the altitude variations of the peak sodium density.

For ESP3, the sodium density variations in both beams are relatively complex. In this case, the fitted altitude variation of the peak sodium density derived from the west beam is used to characterize the evolution of ESP3 in both beams.

Therefore, the black dashed lines are derived from the observed altitude variations of the peak sodium density and serve as guides to illustrate the motion of the ESP features.

5. Line 165, I am not sure including the two digits behind the decimal point, like "2.67", is necessary. I suggest the author to ignore them, because the uncertainty is large. In addition, please use the same unit, either km/hr or m/s, to be consistent throughout the paper.

We have revised the reported numerical values by reducing the number of decimal places from two to one throughout the manuscript. In addition, the velocity unit has been unified to m/s throughout the manuscript for consistency. The corresponding revisions have been made at Line 183 and throughout the text in the revised manuscript.

6. Line 170, the statement "… suggests that the Es layer served as the primary source of SSL1" seems to be too strong (see my comment above). There have been no direct evidence to support this statement.

We agree that the phrase "served as the primary source" may be overly strong. Accordingly, we have revised the relevant statements at Lines 188-189 in the revised manuscript.

As shown in Figure 6c, the Es layer is located approximately 2–3 km above SSL1, suggesting that the two features were closely spaced in altitude. In addition, the Es layer and SSL1 exhibit similar temporal evolution and upward motion. The maximum foEs reached 9.3 MHz during the event, corresponding to an electron density comparable to that reported by Xue et al. (2017). Their chemical model suggests that strong Es layers could provide sufficient metallic ions to produce sodium enhancements on a timescale comparable to that observed for SSL1.

Therefore, our observations are consistent with the hypothesis that the Es layer may have contributed to the formation of SSL1. We agree that the present observations do not provide direct evidence to establish a causal relationship. Accordingly, the statement has been revised from "the Es layer served as the primary source of SSL1" to "the Es layer may have contributed to the formation of SSL1" (Lines 188-189).

7. Line 201, suggesting to replace "are less reliable" with "have large uncertainty"

We have replaced the phrase "are less reliable" with "have large uncertainty" as suggested at Line 219 in the revised manuscript.

8. Line 202-203, are these wind values at the centroid/peak altitude of SSL/ESP? Please clarify.

We have added a clarification at Line 220 in the revised manuscript. The reported wind values do not correspond to the centroid or peak altitude of the SSL/ESP. Instead, they represent the average zonal wind within the temporal and altitude ranges occupied by each SSL or ESP event.

For example, SSL3 extends from 19.5 to 21.0 UT and from 92 to 97 km altitude. The reported wind value (9.7 m/s) is obtained by averaging the zonal wind over this entire time–height region.

9. Line 235-237, see my comment above about the altitude difference and zero-wind line. This statement is questionable. If the Es altitude has to be down shifted by 10 km, the zero-wind line cannot occur within the Es. There could be another zero-wind line above, where the radar cannot reach. Therefore, the contribution from radar is very limited in this investigation.

Thank you for this insightful comment. We would like to clarify that the ~10 km downward shift applied to the Es altitude curve in Figure 9 was only introduced for visual comparison with the reconstructed tidal wind. We have revised the corresponding discussion at Lines 254–256 in the revised manuscript.

In this study, the tidal wind field reconstructed from the meteor radar observations is mainly used to characterize the tidal phase evolution. Since the radar-derived tidal information is available only up to approximately 100 km, it cannot directly demonstrate the physical processes responsible for the observed Es layer variability. Our results show that the overall descending trend of the Es layer is consistent with the phase evolution of the reconstructed tidal winds, suggesting that tidal wind may contribute to the evolution of Es layer. This consistency is considered as supporting evidence rather than direct proof of the Es formation mechanism.

10. Line 250-255, I understand the calculation of the overall uncertainty of the vertical ion drift based on EQ 1 can be a challenging task. However, I would appreciate the author can provide some estimation of the uncertainty of Wiz, because it is important for related discussion followed. If possible, the uncertainty can be added in Figure 9 and 10.

Thank you for this valuable suggestion. We agree that an estimate of the uncertainty in the ion vertical drift (Wiz) is important for evaluating the subsequent discussion.

Following this suggestion, we additionally calculated and plotted Wiz and dWiz/dz in Figure R3 for the purpose of uncertainty evaluation. The corresponding uncertainties of Wiz and dWiz/dz are presented in Figures R4.

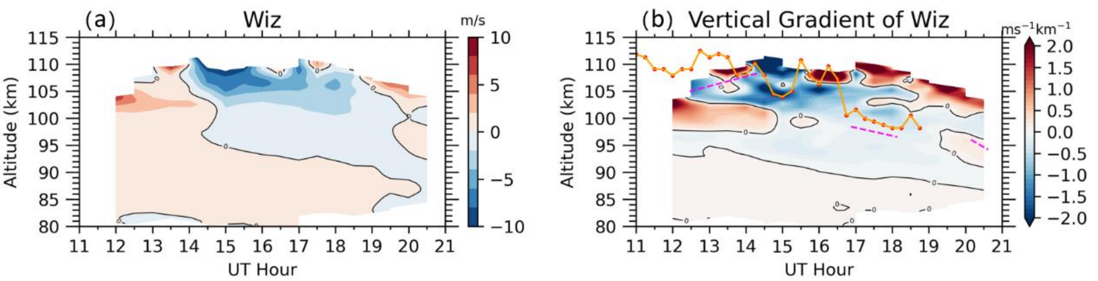

Figure R3. Time–height contour of ion vertical drift (a) and vertical gradient of ion vertical drift (b) derived from zonal wind measured by the USTC sodium lidar on 13 June 2013. Cold colors indicate negative value, while warm colors indicate positive value. In figure (b), The orange line denotes the altitude variation of the Es layer measured by the Wuhan ionosondes, and the dashed purple lines indicate the trajectories of the SSLs.

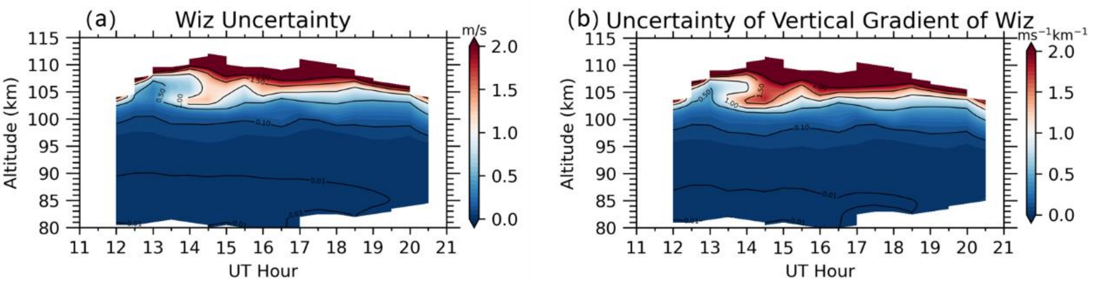

Figure R4. Time–height contours of uncertainty of Wiz (a) and uncertainty of vertical gradient of Wiz (b). Black solid lines represent uncertainty values of 0.01, 0.10, 0.50, 1.0, 1.5, and 2.0.

During this revision, we also re-examined the numerical calculation of the vertical gradient of the ion vertical drift (dWiz/dz). In the previous version, the gradient was approximated as:

$$\frac{dw_{iz}(z)}{dz} = \frac{r_i(z)cosI}{1 + r_i^2(z)} \times \frac{U\left(z + \frac{1}{2}\Delta z\right) - U\left(z - \frac{1}{2}\Delta z\right)}{\Delta z}$$

Where $r_i(z)$ is the ratio of the ion-neutral collision frequency to the ion gyrofrequency at altitude z, and U(z) is the zonal wind at altitude z.

After revisiting the formulation, we adopted a more complete discrete expression by first calculating the ion vertical drift at adjacent altitude levels and then evaluating its vertical gradient:

$$\frac{dw_{iz}(z)}{dz} = \frac{\frac{r_i\left(z + \frac{1}{2}\Delta z\right)cosI}{1 + r_i^2\left(z + \frac{1}{2}\Delta z\right)} \times U\left(z + \frac{1}{2}\Delta z\right) - \frac{r_i\left(z - \frac{1}{2}\Delta z\right)cosI}{1 + r_i^2\left(z - \frac{1}{2}\Delta z\right)} \times U\left(z - \frac{1}{2}\Delta z\right)}{\Delta z}$$

Figure 10 has been recalculated and updated using this revised formulation. Importantly, the revised Figure 10 preserves the principal features identified in the previous version. For example, at approximately 12:30 UT, an ion divergence region near 100 km and an ion convergence region near 105 km still follow the downward progression of the tidal phase. In addition, the two strong ion convergence regions near 104 km (14:30–15:00 UT) and near 105 km (around 16:00 UT) remain evident. Therefore, the principal ion convergence/divergence structures remain robust, and the scientific conclusions of the manuscript are unchanged.

To estimate the uncertainties, we consider only the uncertainty propagation associated with the measured wind uncertainty. The corresponding uncertainties of Wiz and dWiz/dz are given by

$$err(W_{iz}(z)) = |\frac{r_i(z)cosI}{1 + r_i^2(z)}| \times err(U(z))$$

$$err(\frac{dW_{iz}(z)}{dz}) = \frac{\sqrt{[\frac{r_i(z + \frac{1}{2}\Delta z)cosI}{1 + r_i^2(z + \frac{1}{2}\Delta z)} err\left(U\left(z + \frac{1}{2}\Delta z\right)\right)]^2 + [\frac{r_i(z - \frac{1}{2}\Delta z)cosI}{1 + r_i^2(z - \frac{1}{2}\Delta z)} err\left(U\left(z - \frac{1}{2}\Delta z\right)\right)]^2}}{\Delta z}$$

Where err(U(z)) is the uncertainties of zonal wind at altitude z.

Following the interpretation of ion convergence proposed by Xue et al. (2013), negative values of dWiz/dz correspond to ion convergence regions, whereas positive values indicate ion divergence regions. The evolution of the Es layer discussed in the manuscript is primarily interpreted based on the temporal and vertical variations of these ion convergence and divergence regions.

As shown in Figure R4, the estimated uncertainty of Wiz is typically less than 0.1 m/s below 100 km and less than 1.0 m/s below 105 km. The estimated uncertainty of dWiz/dz is typically less than 0.1 m/s/km below 97 km and less than 1.5 m/s/km below 105 km. Comparison of Figures R3–R4 indicates that the estimated uncertainties are overall smaller than the major ion convergence and divergence structures discussed in the manuscript and therefore do not affect the main conclusions.

Since Figures 9 and 10 are contour plots, adding the corresponding uncertainty distributions directly to the figures would substantially reduce their readability. Therefore, we provide the uncertainty estimation and calculation procedure here for reference while retaining the original presentation of Figures 9 and 10 in the revised manuscript.

Reference:

Xue, X. H., Dou, X. K., Lei, J., Chen, J. S., Ding, Z. H., Li, T., Gao, Q., Tang, W. W., Cheng, X. W., and Wei, K.: Lower thermospheric-enhanced sodium layers observed at low latitude and possible formation: Case studies, J. Geophys. Res. Space Physics, 118, 2409–2418, https://doi.org/10.1002/jgra.50200, 2013.

11. Line 321, suggest to replace “coupled” with “likely”

We have replaced “coupled” with “likely” at Line 340 in revised manuscript.

12. Line 328, suggest to replace “indicate” with “suggest”

We have replaced “indicate” with “suggest” at Line 347 in revised manuscript.

Figure captions:

1. Figure 1. I think the white vertical lines are data gaps. If so, please include the related statement in the caption.

We have added statement that “The white vertical lines represent data gaps” in the caption of Figure 1 in the revised manuscript.

2. Figure 4. I think “over 95-100 km height” is referring the altitude range. Please modify.

We have modified the caption of Figure 4 by replacing “over 95–100 km height” with “within the altitude range of 95–100 km” in the revised manuscript.

Response to Referee 2

1. The authors introduce the term "enhanced sodium patterns (ESPs)" but do not provide a clear, objective criterion to distinguish ESPs from SSLs. Please provide a quantitative operational definition for ESPs.

Thank you for this comment. In the revised manuscript (Lines 80-88), we have explicitly defined both SSLs and ESPs. Following Dou et al. (2009), an SSL is identified according to three quantitative criteria: (1) peak sodium density at least twice the background density at the same altitude and exceeding 1000 cm^{-3} above 100 km, (2) FWHM less than 4.0 km, and (3) duration longer than 15 min in the present study (adjusted from the original criterion because our lidar has a temporal resolution of 1 min).

An ESP is defined as a distinct sodium density enhancement event that does not satisfy one or more of the SSL identification criteria.

For example, ESP3 does not satisfy the first criterion because its peak sodium density is less than twice the background sodium density at the corresponding altitude. Therefore, it is classified as an ESP rather than an SSL.

Reference:

Dou, X. K., Xue, X. H., Chen, T. D., Wan, W. X., Cheng, X. W., Li, T., Chen, C., Qiu, S., and Chen, Z. Y.: A statistical study of sporadic sodium layer observed by Sodium lidar at Hefei (31.8° N, 117.3° E), Ann. Geophys., 27, 2247–2257, https://doi.org/10.5194/angeo-27-2247-2009, 2009.

2. The propagation delays for ESPs are estimated by visually aligning phase lines, no uncertainty estimates are provided. Please provide a more objective cross-correlation analysis between the east and west beam time series, with uncertainty quantification. This is essential for the horizontal transport discussion.

Thank you for this valuable suggestion. The procedure for determining the black dashed lines in Figure 5 was not sufficiently described in the original manuscript. We have modified and added a description of the procedure for identifying at Lines 169-173 and the caption of Figure 5 in the revised manuscript.

The cross-correlation method suggested by the referee provides an objective approach for estimating time delays between two continuous signals. We carefully considered this method and re-examined the ESP events investigated in this study. Since the ESPs are isolated sodium enhancement events with distinct vertical structures, we found that the propagation delays can be effectively determined by tracking the temporal evolution of the sodium density peak altitudes in the east and west beams. This peak-altitude tracking method directly characterizes the movement of individual ESP structures and provides a quantitative estimate of their propagation delays.

As illustrated in the Figure R5 below, the black dashed lines in Figure 5 are determined from the identified sodium density peak altitudes rather than manually adjusted. At each observation time, the altitude corresponding to the maximum sodium density within the ESP structure is identified, and these peak-altitude points are connected to represent the evolution of the ESP. For ESP1 and

ESP3, where the sodium density variations in one of the beams are relatively complicated, the peak-altitude trajectories are obtained by fitting the identified peak positions to better represent the overall evolution of the events. For ESP2, the black dashed lines are directly determined from the identified sodium density peak altitudes. The propagation delays are then calculated from the temporal offsets between the corresponding peak-altitude trajectories observed in the east and west beams.

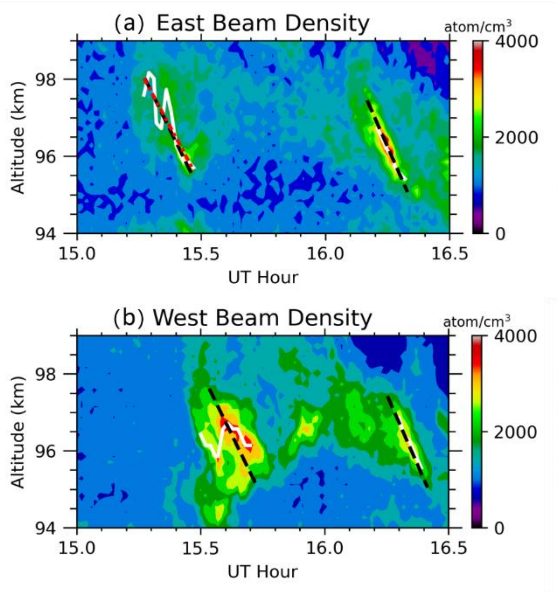

Figure R5. Time–height contours showing the detailed structures of ESP1 and ESP2 (a, b) and ESP3 (c, d) observed by the east beam (a, c) and west beam (b, d). The white solid lines indicate the altitude variations of the maximum sodium density during each ESP event. The red dotted lines represent linear fits to the white solid lines. The black dashed lines correspond to the trajectories presented in Figure 5 of the manuscript and closely follow the red dotted lines, suggesting that they could be used to illustrate the evolution of the ESP features.

3. In Section 5.2, the tidal reconstruction is useful for illustrating tidal control, but the ion convergence calculation (Figure 10) already uses lidar zonal wind. The connection between the two approaches is not clearly explained. Please clarify the added value of the tidal reconstruction and why the lidar wind is not used for the zero-wind comparison in Figure 9.

We agree that the relationship between the tidal reconstruction and the ion convergence analysis should be clarified. In this study, the reconstructed tidal wind (Figure 9) and the lidar-measured zonal wind used for the ion convergence calculation (Figure 10) are used to investigate the role of atmospheric winds in Es-layer evolution at different temporal scales.

The tidal reconstruction using the meteor radar zonal wind is designed to investigate the possible tidal influence on the Es layer. By reconstructing the diurnal and semidiurnal tidal components, the influence of short-period disturbances, such as gravity waves, is largely removed, helping to identify the possible tide influence on Es-layer variations.

Meanwhile, the ion convergence calculation uses the high-temporal-resolution zonal wind measured by the lidar to investigate the fine-scale dynamical processes responsible for the observed Es evolution. The lidar wind captures short-term convergence and divergence transitions that closely correspond to the observed perturbations and rapid descent of the Es layer, providing a more detailed interpretation of the observed structures.

The lidar wind was not used for the tidal reconstruction in Figure 9 because the lidar observations cover only approximately 9 hours, which is insufficient for reliably separating the diurnal and semidiurnal tidal components. In contrast, the meteor radar provides continuous wind measurements over a full day and therefore enables a more robust tidal reconstruction.

Therefore, the meteor radar tidal reconstruction provides information on the tidal phase evolution, whereas the lidar wind is used to investigate the detailed ion convergence associated with the observed Es evolution. These two analyses are complementary and together provide a more comprehensive understanding of the relationship between the wind field and Es-layer dynamics. We appreciate the referee’s comment, which helped us clarify the different purposes and added value of these two approaches.

4. In discussion, the statement that GWs may induce a downward vertical phase shift of the Es layer over Hefei (Page 15) is speculative. Please provide a physical or modeling basis for this, or rephrase as a hypothesis.

Thank you for this comment. The previous statement regarding the potential role of gravity waves in causing a downward phase shift of the Es layer was speculative, as no direct modeling results or quantitative evidence were provided. We have modified the sentence at Lines 329-331 in the revised manuscript to clarify that gravity-wave-induced vertical phase variations may contribute to differences in Es-layer altitude between the Wuhan and Hefei, which is proposed as a hypothesis rather than a demonstrated mechanism.